Int. J. Solids Structures Vol. 29, No. 7, pp. 879–891, 1992
Printed in Great Britain.

0020–7683/92 $5.00+.00

ON THE ANALYSIS OF PRISMATIC BEAMS USING FIRST-ORDER WARPING FUNCTIONS

C. A. IE† and J. B. KOSMATKA‡
Department of Applied Mechanics and Engineering Science, University of California, La Jolla, California 92093, U.S.A.

(*Received* 14 *September* 1990; *in revised form* 27 *June* 1991)

Abstract—A one-dimensional theory for isotropic homogeneous beams with a general cross-section is developed that utilizes both deformations in the cross-section plane and warping out of the cross-section plane where these deformation functions are known from Saint-Venant's elasticity solutions for bending and flexure of a prismatic beam (first-order warping functions). In contrast to existing technical beam theories which assume that local cross-section deformations and some stresses can be neglected, the present theory makes no assumption. The finite element model is developed using the resulting differential equations along with a partially weak-form formulation. Full three-dimensional constitutive equations are used. Solutions are found using the finite element method. Numerical results, which are presented for a wide variety of loadings and boundary conditions, show that the calculated stresses and displacements are in excellent agreement with existing elasticity solutions.

INTRODUCTION

Without a loss of generality, consider a prismatic beam of length L and characteristic height h that is composed of a homogeneous isotropic material. The beam is subjected to a transversely distributed load $p(z)$ that acts along the beam surface (line $x = 0, y = \bar{y}, z$). For additional details see Fig. 1. Existing technical (one-dimensional) beam theories [for example Love (1927)], have been developed based upon the assumption that the three stresses within the cross-section are small and can be neglected. Classical beam theory (commonly called a Bernoulli–Euler beam theory) further assumes simple kinematical relations with respect to the displacement fields, i.e. plane sections perpendicular to the undeformed axis remain plane and perpendicular to the deformed axis. As a consequence, the two remaining transverse shear stresses (as a result of zero shear strains) also vanish. Hence, the complete description of the beam deformation is determined using the remaining normal stress where the strain energy of the beam includes only bending effects. For long slender isotropic beams ($L/h > 10$), it is well known that the strain energy due to shear is negligibly small compared to bending, thus the Bernoulli–Euler approach leads to a suitable representation of gross structural behavior.

As the geometric aspect ratio (L/h) gets smaller, the ratio of the shear strain energy to bending strain energy becomes significant and the effects of transverse shear deformation cannot be ignored. Timoshenko (1921, 1922) developed a beam theory that accounts for transverse shear deformation based on the assumption that plane sections perpendicular to the undeformed axis remain perpendicular after deformation. Since the assumption that plane sections remain plane after deformation still holds, the resulting transverse shear strains (and corresponding shear stresses) are constant throughout the cross-section, thus violating the requirement of a stress-free boundary condition on the lateral boundaries. A shear correction factor (k) is introduced to improve the model's global displacement behavior, where this factor is dependent upon the section shape, material definition, and load type. Unfortunately, there are as many estimates of (k) for a given cross-section, as there are definitions for their existence [for example Cowper (1966) and Kaneko (1975)], and the resulting displacement solutions are sensitive to the selected (k) value.

Recently, Levinson (1981), Heyliger and Reddy (1988) and Kant and Gupta (1988) developed theories that more accurately represent the kinematical relations of a transversely

†Graduate research assistant.
‡Assistant Professor.

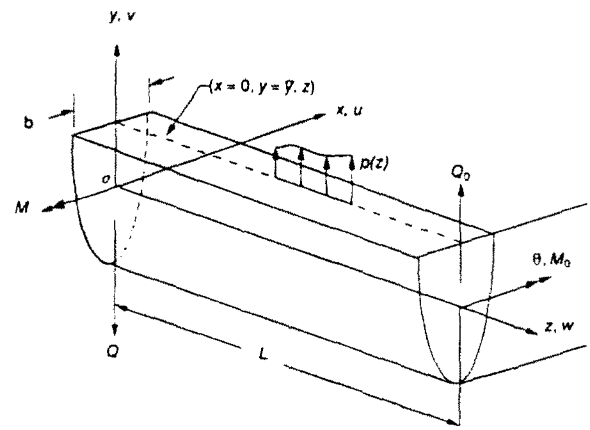

Fig. 1. A beam with its reference axes.

loaded shear deformable beam. These theories, which are commonly called "Higher Order Theories", are capable of modeling the parabolic distribution of the transverse shear stresses through the thickness which is needed to satisfy the stress-free boundary conditions on the lateral surfaces. Thus, a shear correction factor is not needed. This approach is limited to simple beams with thin rectangular cross-sections, because of the difficulty of defining the kinematic displacement field for a general cross-section. This approach has been extended, by Reddy (1984), to the analysis of plates.

Beam theories that include the warping of the cross-section as a result of applied transverse loads have also been developed. Vlasov (1961) developed a model that includes the out-of-plane warping for thin-walled isotropic beams having simple cross-sections (circular tubes, I-beams, rectangular box beams). Bauchau (1985) extended this approach for thin-wall composite beams where eigen-warping functions are used to model the out-of-plane shear-dependent warping.

Analytical models have also been developed for determining the in-plane cross-section deformations and out-of-plane warping of a beam with an arbitrary cross-section subjected to bending and tip shear loads (Saint-Venant's bending and flexure problems). These solutions, which are based upon solving a coupled two-dimensional elasticity problem, have been developed for arbitrary cross-sections composed of isotropic materials by Mason and Herrmann (1968), a restricted class of orthotropic materials by Wörndle (1982), and generally anisotropic materials by Kosmatka and Dong (1991).

The cross-section warping (both in- and out-of-plane) and stress distribution depend not only upon the geometry and the material definition, but also on the type of loading. The description of the warping function becomes increasingly more complex as the applied loading changes from simple end loadings to non-uniform distributed loads. Furthermore, this description also becomes more complex if one tries to study higher vibrational (short wavelength) modes because of the change in shear stress distribution with mode number [see Goodman and Sutherland (1951) for details]. But for most beam-type structures there is a class of warping functions that are dominant. These functions are defined as first-order functions and their magnitudes are linearly proportional to the local stress resultants.

For the sake of simplicity and clarity, the following theory is developed for an isotropic beam having a general cross-section subjected to arbitrary transverse loadings. It can easily be extended to the analysis of more complex material definitions as long as one can obtain the requisite first-order warping functions. In this study, a set of numerical examples is presented to fully verify the current approach by studying a beam with a rectangular cross-section subjected to a wide variety of boundary conditions and loadings. The selected warping functions for the isotropic homogeneous rectangular cross-section were derived from Sokolnikoff (1956). The out-of-plane function represents the warping of the cross-section as a result of an applied transverse tip load (Saint-Venant flexure problem) and the in-plane function represents the anticlastic surface that results from an applied bending moment (Saint-Venant bending problem).

THEORETICAL DEVELOPMENT

Consider a prismatic beam composed of an isotropic homogeneous material having a general cross-section (see Fig. 1). A Cartesian coordinate system (x, y, z) is defined on the beam where x and y are coincident with the principal axes of the root cross-section and z is coincident with the line of centroids. The beam is subjected to both transverse distributed loadings (p) and end loads (Q_0, M_0) in the y–z plane. The displacement distributions in the x-, y- and z-directions are defined as

$$\tilde{u}(x, y, z) = M(z)U_0(x, y),$$
$$\tilde{v}(x, y, z) = v(z) + M(z)V_0(x, y),$$
$$\tilde{w}(x, y, z) = y\theta(z) + Q(z)W_0(x, y), \tag{1a–c}$$

where $v(z)$ and $Q(z)$ represent the displacement and local shear force in the y-direction, respectively; $\theta(z)$ and $M(z)$ represent the rotation and local moment about the x-axis, respectively, and $U_0(x, y)$, $V_0(x, y)$ and $W_0(x, y)$ are the functions associated with the in-plane and out-of-plane warping definition, respectively. These last three functions, which are assumed to be known, can be determined for a given cross-section by solving Saint-Venant's elasticity problems for bending and flexure [see Mason and Herrmann (1968), Wörndle (1982) and Kosmatka and Dong (1991)]. The units associated with these three functions must be defined carefully so that when they are multiplied by the appropriate stress resultant, the resulting product has units of length.

The strain–displacement relationships of the beam are defined as

$$\varepsilon_x = \tilde{u}_{,x},\quad \varepsilon_y = \tilde{v}_{,y},\quad \varepsilon_z = \tilde{w}_{,z},\quad \gamma_{yz} = \tilde{v}_{,z} + \tilde{w}_{,y},\quad \gamma_{xz} = \tilde{w}_{,x} + \tilde{u}_{,z},\quad \gamma_{xy} = \tilde{u}_{,y} + \tilde{v}_{,x}, \tag{2a–f}$$

where ε_x, ε_y and ε_z are the normal strains in the x-, y- and z-directions, respectively, and γ_{yz}, γ_{xz} and γ_{xy} are the shear strains. The notation $(\ )_{,x}$ and $(\ )_{,y}$ refer to partial derivatives with respect to the x and y coordinates respectively. The general constitutive relations are given as

$$\{\sigma\} = [C]\{\varepsilon\}, \tag{3a}$$

where the stress and strain arrays are defined as

$$\{\sigma\}^T = \{\sigma_x, \sigma_y, \sigma_z, \tau_{yz}, \tau_{xz}, \tau_{xy}\},$$
$$\{\varepsilon\}^T = \{\varepsilon_x, \varepsilon_y, \varepsilon_z, \gamma_{yz}, \gamma_{xz}, \gamma_{xy}\}, \tag{3b,c}$$

and the material stiffness matrix is given as

$$[C] = \begin{bmatrix} (\lambda+2G) & \lambda & \lambda & 0 & 0 & 0 \\ \lambda & (\lambda+2G) & \lambda & 0 & 0 & 0 \\ \lambda & \lambda & (\lambda+2G) & 0 & 0 & 0 \\ 0 & 0 & 0 & G & 0 & 0 \\ 0 & 0 & 0 & 0 & G & 0 \\ 0 & 0 & 0 & 0 & 0 & G \end{bmatrix}. \tag{3d}$$

Here, λ and G are defined as Lamé's constants.

The bending moments and shear forces in the cross-section are defined as

$$M(z) = \int_A y\sigma_z \, dA, \quad Q(z) = \int_A \tau_{yz} \, dA \tag{4a,b}$$

where A is the area of the cross-section.

To be consistent with using only the first-order warping functions (while neglecting the higher-order functions), the variation in the shear forces over the beam length, which must be equal to the applied transverse loads (due to the elemental equilibrium in the y-direction), is set equal to zero. This assumption is made so that the displacement field can be expressed in terms of kinematical variables only, instead of the mixed formulation of (1a–c). Thus,

$$Q' = -p(z) = 0, \tag{5}$$

where prime denotes the derivative with respect to z. Using eqns (1)–(5) one can express the bending moment about the principal axes as

$$M(z) = \tilde{E}I\theta', \tag{6a}$$

where

$$\tilde{E} = \frac{(\lambda + 2G)}{1 - \lambda H_1}, \tag{6b}$$

$$H_1 = \int_A y(U_{0,x} + V_{0,y}) \, dA, \tag{6c}$$

and I is the area moment of inertia about the x-axis. For homogeneous isotropic cross-sections, the functions U_0 and V_0 are required to satisfy: $U_{0,x} = V_{0,y} = -\nu y/EI$ (from Saint-Venant's plane strain bending problem), and thus H_1 reduces to $-2\nu/E$ and $\tilde{E} = E$.

Similarly, using eqns (4b) and (3) the local shear force Q can be written as

$$Q = G\int_A \gamma_{yz} \, dA, \tag{7a}$$

or it can be defined by making use of eqns (2d) and (1) as

$$Q = G\int_A \{(v' + \theta) + M'V_0 + QW_{0,y}\} \, dA \tag{7b}$$

and M' can be replaced by Q. Solving for Q:

$$Q = k_0 GA(v' + \theta) \tag{7c}$$

where

$$k_0 = \frac{1}{(1 - GH_2)} \tag{7d}$$

and

$$H_2 = \int_A (V_0 + W_{0,y}) \, dA. \tag{7e}$$

Substituting eqns (6) and (7) into eqn (1) results in the final form of the displacement relations defined in terms of the kinematic variables (v and θ) only:

$$\tilde{u}(x,y,z) = \theta'\psi_x(x,y),$$
$$\tilde{v}(x,y,z) = v+\theta'\psi_y(x,y),$$
$$\tilde{w}(x,y,z) = y\theta+(v'+\theta)\psi_z(x,y) \tag{8a–c}$$

where

$$\psi_x(x,y) = \tilde{E}IU_0(x,y),$$
$$\psi_y(x,y) = \tilde{E}IV_0(x,y),$$
$$\psi_z(x,y) = k_0GAW_0(x,y). \tag{9a–c}$$

This displacement field will be used as the basis for the remaining development, where no limiting assumptions are made corresponding to load type.

EQUILIBRIUM EQUATIONS

The two equations of equilibrium for the beam are determined by applying the principle of virtual work

$$\delta U - \delta W_e = \int_0^L \int_A \{\sigma\}^T\{\delta\varepsilon\}\,dA\,dz - \int_0^L p\delta v_a\,dz = 0 \tag{10}$$

where v_a represents the displacement on the surface of the beam at the point of the applied load $[v(x=0, y=\bar{y})]$. The resulting differential equations are

$$Q'+p-S_1''+S_2' = 0 \tag{11a}$$

$$M'-Q+S_1'-S_2+S_3'-S_4''-p'\overline{\psi_y} = 0 \tag{11b}$$

where $\overline{\psi_y}$ is the magnitude of the warping displacement at the point of the applied load given as:

$$\overline{\psi_y} = \psi_y(x=0, y=\bar{y}) \tag{11c}$$

and the force and moment resultants (S_1 through S_4) are defined in the Appendix (eqns A1–A4). From the above equilibrium equations (11a,b) it is readily apparent that for an isotropic homogeneous beam subjected to a concentrated flexure load at the tip, the resultants must satisfy: $S_1'' = S_2'$ and $S_3'' = S_4'''$. Similarly, for a uniformly distributed load: $S_1''' = S_2''$ and $S_3''' = S_4''''$, and for a linearly varying distributed load: $S_1'''' = S_2'''$ and $S_3'''' = S_4'''''$. For rectangular cross-sections, it further holds that for a tip loaded beam (constant shear) that: $S_3' = S_4'' = 0$, for a uniformly distributed load that: $S_3'' = S_4''' = 0$, and for a linearly varying distributed load that: $S_3''' = S_4'''' = 0$. Alternatively, the above equilibrium equations can be written in terms of the kinematic variables (v, θ) as

$$D_{22}v'''' - A_{11}(v'+\theta') - (A_{12}-D_{12})\theta - p = 0 \tag{12a}$$

$$A_{22}\theta'''' - (D_{11}-2A_{12})\theta'' + A_{11}(v'+\theta) + (A_{12}-D_{12})v''' + p'\overline{\psi_y} = 0 \tag{12b}$$

where A_{ij} and D_{ij} $(i,j = 1,2)$ are shear stiffness and bending stiffness constants, respectively, that are defined in the Appendix (eqns A5 through A10). There are four necessary sets of boundary conditions that must be specified at the beam root and tip. First, either the transverse displacement (v) or the effective shear force:

$$\tilde{Q} = Q - S_1' + S_2, \tag{13a}$$

must be defined. Second, either the derivative of the transverse displacement (v') or the out-of-plane warping-based work done (S_1) must be specified. Third, either the rotation θ or the effective bending moment:

$$\tilde{M} = M + S_1 + S_3 - S_4' - p\overline{\psi}_v, \tag{13b}$$

must be specified. Lastly, either the derivative of the rotation θ' or (S_4) must be defined.

FINITE ELEMENT MODEL

One could use the principle of stationary potential energy to develop a finite element representation of the above equations. The problem that is encountered though, is the incorporation of the four boundary conditions. Unfortunately, some of these conditions are not physically meaningful. Hence, in this paper, a variational (or partially weak) formulation is used to develop the finite element equations where the governing equations (eqn 11) are used and integration by parts is performed only once to get the necessary recognized terms, such as transverse displacements (v), rotations (θ), shear forces and moments. As a consequence, the stiffness matrix is non-symmetric.

The beam is divided into a series of subregions where the kinematic variables (v, θ) for each subregion are represented by approximate functions of the form

$$v = \sum_{i=1}^{m} \phi_{v_i} V_i, \quad \theta = \sum_{j=1}^{n} \phi_{\theta_j} \Theta_j, \tag{14a,b}$$

where V_i and Θ_j are nodal displacements and rotations, respectively, and ϕ_{v_i} and ϕ_{θ_j} are continuous fully differentiable functions with respect to z. Writing the variational form of the two governing equations as

$$0 = \int_0^L \phi_{v_i}[Q' + p - S_1'' + S_2']\,\mathrm{d}z; \quad i = 1, \ldots, m$$

$$0 = \int_0^L \phi_{\theta_j}[M' - Q + S_1' - S_2 + S_3' - S_4'' - p'\psi_v]\,\mathrm{d}z; \quad j = 1, \ldots, n \tag{15a,b}$$

where the expressions in the brackets are the equilibrium equations from eqns (11a,b). The following expressions are defined by integrating the above functionals by parts once:

$$\int_0^L \phi_{v_i}' Q\,\mathrm{d}z + \int_0^L \phi_{v_i}(S_1'' - S_2')\,\mathrm{d}z = Q\phi_{v_i}|_0^L + \int_0^L \phi_{v_i} p\,\mathrm{d}z$$

$$\int_0^L \phi_{\theta_j}' M\,\mathrm{d}z + \int_0^L \phi_{\theta_j}(Q - S_1' + S_2 - S_3' + S_4'')\,\mathrm{d}z = \phi_{\theta_j} M|_0^L - \int_0^L \phi_{\theta_j} p'\overline{\psi}_v\,\mathrm{d}z. \tag{16a,b}$$

A finite element formulation is obtained by expressing the stress-dependent constants (M, Q, S_1–S_4) in terms of the kinematic variables (v, θ) of eqn (14a,b) using eqns (3a–d), (2a–f) and (8a–c). In matrix form, the model can be written as

$$\begin{bmatrix} [K_{vv}] & [K_{v\theta}] \\ [K_{\theta v}] & [K_{\theta\theta}] \end{bmatrix} \begin{Bmatrix} \{V\} \\ \{\Theta\} \end{Bmatrix} = \begin{Bmatrix} \{F_v\} \\ \{F_\theta\} \end{Bmatrix} + \begin{Bmatrix} \{f_v\} \\ \{f_\theta\} \end{Bmatrix}, \tag{17}$$

where $\{V\}$ and $\{\Theta\}$ are mth and nth order one-dimensional arrays that contain the unknown nodal displacements and rotations from eqn (14a,b), respectively, $\{F_v\}$ and $\{F_\theta\}$ and mth and nth order one-dimensional arrays that contain the applied nodal forces and moments, respectively, and the remaining sub-matrices are defined in the Appendix (eqns A11–A15).

NUMERICAL EXAMPLES AND DISCUSSION

Numerical examples are presented to illustrate the accuracy of the current approach in comparison with existing models (full three-dimensional elasticity, plane-stress elasticity, Timoshenko beam theory, and Bernoulli–Euler theory). Displacement and stress distributions are examined for an isotropic homogeneous beam with a rectangular cross-section as a function of beam length [from short deep ($L/h = 3$) to long slender ($L/h = 20$)] for three different load/boundary configurations. The warping functions for a rectangular cross-section are determined using a full three-dimensional elasticity solution [from Sokolnikoff (1956)] as

$$U_0(x, y) = -\frac{\nu}{EI}xy, \tag{18a}$$

$$V_0(x, y) = -\frac{\nu}{2EI}(y^2 - x^2), \tag{18b}$$

$$W_0(x, y) = -\frac{1}{EI}\left\{\frac{2+\nu}{6}y^3 - \frac{\nu}{2}yx^2 + \frac{\nu b^2}{\pi^3}\sum_{n=1}^{\infty}\frac{(-1)^n\left(\frac{b}{2}\sinh\left(\frac{2n\pi y}{b}\right)\cos\left(\frac{2n\pi x}{b}\right) - n\pi y\right)}{(n^3)\cosh\left(\frac{n\pi h}{b}\right)}\right\} \tag{18c}$$

where b and h represent the cross-section width and height in the x- and y-directions respectively, I is the cross-section area moment of inertia and E and ν are defined as the Young's modulus and Poisson ratio (taken equal to 0.25) of the material, respectively.

The value of (k_0) for a rectangular cross-section can be determined by substituting eqns (18b,c) into (7c), carrying out the integration, and then substituting the resulting value for H_2 into eqn (7d):

$$k_0 = \frac{1}{1 + \frac{1}{2(1+\nu)}\left\{1 + \nu\left(1 - \frac{b^2}{h^2}\right) - \frac{12\nu b^2}{\pi^2 h^2}\sum_{n=1}^{\infty}\frac{(-1)^n}{n^2}\frac{1}{\cosh\left(\frac{n\pi h}{b}\right)}\right\}}. \tag{19}$$

This coefficient (k_0) will approach 2/3 for very thin rectangular cross-sections ($b/h \approx 0$) or for negligible Poisson's ratios ($\nu \approx 0$). The variation of k_0, along with A_{ij} and D_{ij} ($i, j = 1, 2$), for a variety of cross-section aspect ratios is presented in Table 1, where the section shear and bending stiffnesses have been non-dimensionalized. These results clearly show how

Table 1. Non-dimensionalized values of A_{ij} and D_{ij} for various rectangular cross-section aspect ratios (h/b)

h/b	400	100	10	1	1/3	1/5
A_{11}/GA	0.562	0.562	0.562	0.587	0.395	0.716
A_{12}/GAh^2	−0.0048	−0.0048	−0.0047	0.0017	0.0317	−0.182
A_{22}/GAh^4	0.0002	0.0002	0.0002	0.0006	0.0180	0.128
D_{11}/EI_{xx}	0.686	0.686	0.687	0.714	0.463	0.732
D_{12}/EI_{xx}	−0.134	−0.134	−0.134	−0.122	−0.173	0.749
D_{22}/EI_{xx}	0.0463	0.0463	0.0462	0.0409	0.191	1.765
k_0	0.6667	0.6667	0.6671	0.7090	0.8155	0.8301

quickly the constants converge for thin cross-sections. The desired form of the warping functions (ψ_x, ψ_y, ψ_z) from eqns (8a–c) can be determined by substituting eqns (18) and (19) into (9a–c). Thus,

$$\psi_x = -\nu xy, \tag{20a}$$

$$\psi_y = \frac{-\nu}{2}(y^2 - x^2), \tag{20b}$$

and ψ_z is found using eqn (9c), where k_0 and W_0 are defined in eqns (19) and (18c), respectively.

It is interesting to note that the kinematic relations (eqns 8a–c) for this rectangular cross-section reduce identically to both the beam kinematic relations of Levinson (1981) if the rectangular cross-section is assumed to be very thin and to the cylindrical bending displacement distributions described by the refined higher-order plate theory [see Reddy (1984)] by setting $\nu = 0$. Thus

$$\tilde{u} = 0,$$

$$\tilde{v} = v,$$

$$\tilde{w} = y\left[\theta - \frac{4}{3}\left(\frac{y}{h}\right)^2(\theta + v')\right], \tag{21a–c}$$

where $\psi_x = \psi_y = 0$ and $\psi_z = -(4y^3)/(3h^2)$.

The finite element model is developed using Lagrangian polynomials, where the displacement in the y-direction (v) is represented by a fifth-order function using six equi-spaced nodes and the rotation (θ) is represented by a fourth-order function using five equi-spaced nodes. The displacement polynomial was selected as one order higher than the rotation polynomial in order to eliminate any potential "shear-locking" problems for long slender beams [see Tessler and Dong (1981)]. Other higher-order polynomials could be selected, but the current set of polynomials represents the minimum order needed to ensure that all terms are properly represented. This element was fully numerically integrated using Gaussian quadrature and numerical studies verified that there was no evidence of "shear-locking" even for extreme aspect ratios ($L/h \geqslant 1000$). The following numerical results were obtained using only one element. Additional convergence-type studies, using more elements were performed, which showed that the one element solution is correct. Clearly, if more complicated beam-type structures are analyzed, then one would model these structures using an assembly of the current elements. For results obtained using the Timoshenko beam theory, the same element definition (fourth- and fifth-order Lagrangian polynomials) was selected in order to be consistent with the present model. Two values of the shear correction factor (2/3 and 0.8475) were examined.

The three analytical studies that were considered included: a cantilever beam with a square cross-section subjected to a transverse tip-load, a simply-supported beam with a very thin cross-section ($h/b = 400$) acted upon by a distributed load, and a cantilever beam with a very thin cross-section ($h/b = 400$) subjected to a linearly varying distributed load. The thin cross-section was selected for the latter two studies, so that the current model could be directly compared with the plane-stress elasticity solutions of Timoshenko and Goodier (1970). Results are presented for the maximum transverse displacement (v/v_{BE}) as a function of beam length (L/h), where (v_{BE}) is the Bernoulli–Euler prediction for the same aspect ratio, load and location. In addition, the calculated transverse shear stress distributions (τ_{yz}/τ_{yz}-elasticity) as a function of the location within the cross-section ($2y/h$) are presented for an extremely deep beam ($L/h = 4$), where (τ_{yz}-elasticity) is the elasticity shear stress at the section centroid ($x = y = 0$) of the same (z) location.

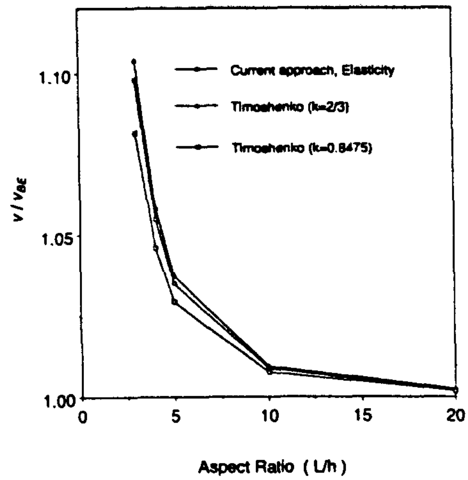

Fig. 2. Tip displacement of a tip-loaded cantilever beam.

Cantilever beam with a transverse tip load

As an initial study, the beam was fixed ($v = \theta = 0$) at the root ($z = 0$) and a concentrated flexure load Q_0 was applied at the tip ($z = L$). In Fig. 2, the predicted tip displacements are presented as a function of the beam length aspect ratio for the current approach, the elasticity solution, the Timoshenko beam theory, and the Bernoulli–Euler beam theory. All of the models are in exact agreement for long slender beams ($L/h \geqslant 20$) where the strain energy associated with the transverse shear stresses is negligible in comparison to the bending stresses. For extremely short deep beams ($3 \leqslant L/h \leqslant 10$), the current model is in exact agreement with the three-dimensional elasticity solution of Sokolnikoff (1956), whereas the Timoshenko-based predictions either slightly over-predict or under-predict the elasticity results depending on whether ($k = 2/3$) or ($k = 0.8475$), respectively.

The non-dimensionalized transverse shear stresses as a function of location within the cross-section (at $x = 0$ and $x = \pm b/2$, $-h/2 \leqslant y \leqslant h/2$) are presented in Fig. 3, for the current model, the elasticity solution and the Timoshenko beam theory. The predicted parabolic shear stress distribution using the current model agrees exactly with the existing elasticity solution at all x- and y-value locations, whereas the constant shear stress distribution calculated using the Timoshenko theory is well known to be incorrect. The magnitude of the Timoshenko predicted shear stresses, which are actually independent of the chosen value of the shear correction factor (k), are equal to the average shear stress Q_0/A where A is the cross-section area. Furthermore, all of the previously mentioned higher-order theories (Levinson, 1981; Heyliger and Reddy, 1988; and Kant and Gupta, 1988)

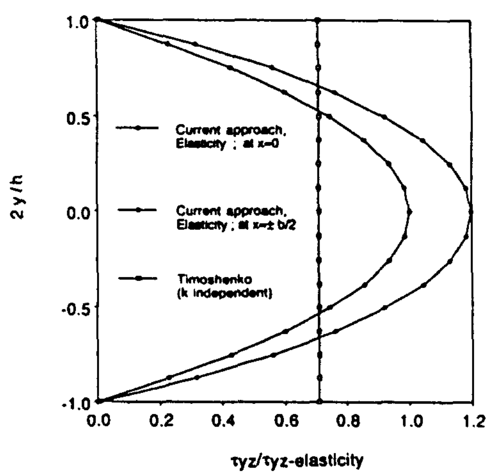

Fig. 3. Transverse shear stress distribution at the root of a tip-loaded cantilever beam.

will only predict the exact shear stress distribution on the y–z plane that passes through the centroid ($x = 0$) because they do not properly account for the x-dependency in the displacement field

Simply-supported beam with a uniformly distributed load

A second study was performed where the boundary conditions for the beam ends ($z = 0, L$) were defined as simply supported ($v = 0$) and the applied load is uniformly distributed along the beam length. The cross-section of the beam was chosen to be very thin ($h/b = 400$) so that the current results could be directly compared to the plane-stress elasticity solutions of Timoshenko and Goodier (1970). The non-dimensionalized displacements at the beam mid-length as a function of beam length aspect ratio are presented in Fig. 4 for the four different models. For long slender beams ($L/h \geqslant 20$), all four of the models agree since the strain energy associated with the shear stresses can be neglected. For extremely short deep beams ($L/h \leqslant 5$), the current model and the Timoshenko beam theory with $k = 0.8475$ predict mid-length displacements that are slightly greater (more flexible) than the plane-stress elasticity solution. These results are excellent considering the severity of the beam length aspect ratio and the fact that the results from the current approach were obtained using the (first-order) warping description obtained from Saint-Venant's flexure problem (tip-loaded beam). Thus, proving that the added displacements effects associated with the higher-order warping functions are negligible in comparison to the first-order warping functions for uniformly loaded beams. This agrees with the theory developed by Michell (1901), which assumes that the analysis of a uniformly loaded beam reduces to a plane strain problem if the warping displacement from Saint-Venant's flexure problem is known. It is interesting to note that although Timoshenko's theory with $k = 2/3$ almost exactly predicts the displacements for a tip-loaded cantilever beam (see above), it over-predicts the displacements in this example. Furthermore, using a value of $k = 0.8475$ gives nearly the exact plane-stress elasticity solution.

As in the case of a cantilever beam with a transverse tip load, an identical figure (see Fig. 3) is obtained for the non-dimensionalized transverse shear stresses at $x = 0$. The parabolic distribution predicted by the current model is in perfect agreement with the plane-stress elasticity solution of Timoshenko and Goodier (1970), while the constant stress distribution predicted using the Timoshenko theory is incorrect and independent of the selected shear correction factor (k).

Cantilever beam with linearly varying distributed load

A final study was performed using an extremely short deep beam ($L/h = 4$) fixed ($v = \theta = 0$) at the root ($z = 0$) and subjected to a linearly varying distributed load with vanishing intensity at the tip. Again, the beam has a very thin cross-section ($h/b = 400$) so

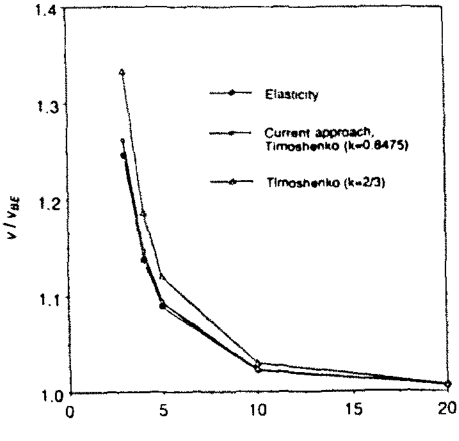

Fig. 4. Mid-length displacement of a simply-supported beam subjected to a uniform distributed load.

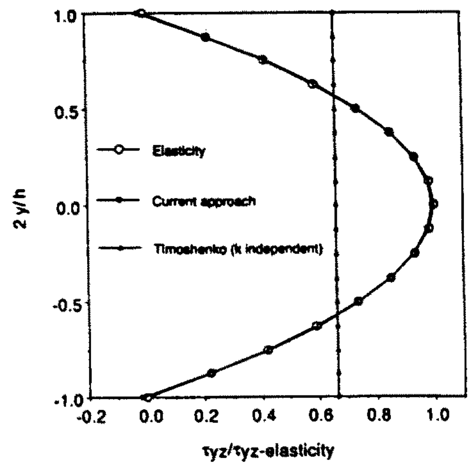

Fig. 5. Transverse shear stress distribution at $z = 3\,L/4$ of a cantilever beam subjected to a linearly varying distributed load.

that direct comparison with the plane-stress elasticity solutions of Timoshenko and Goodier (1970) can be made. The non-dimensionalized shear stress distribution over the section height ($x = 0$, $-h/2 \leqslant y \leqslant h/2$) at z equals $3L/4$ is presented in Fig. 5. Additional shear stress distributions for ($0 \leqslant z \leqslant L/2$) were calculated and found to be in exact agreement with the plane-stress elasticity solutions (i.e. identical to Fig. 3 at $x = 0$). The current model behaves surprisingly well considering that the beam should behave more like a three-dimensional solid than a one-dimensional beam and thus from Saint-Venant's principle the current approach should not be valid in this region. Generally speaking, the current model tries to best approximate the solution in the integral sense.

Although it is possible to extend the current model by incorporating additional higher-order warping functions, it does not appear to be necessary even for short deep beam-type structures. Higher-order warping functions may play an important role for beams with extremely low aspect ratios (closer to solid structures than beam structures) or for higher vibrational modes.

CONCLUSION

A one-dimensional beam theory has been developed that accurately predicts the three-dimensional displacement and stress distribution in homogeneous beams with a general cross-section. The displacement field is developed using the standard kinematic relations to describe the global beam behavior supplemented with an additional field that represents the local deformation within the cross-section and warping out of the cross-section plane. It was assumed that the magnitude of this additional field is directly proportional to the local stress resultants. The current displacement field has been shown to reduce exactly to existing higher-order beam theories that have been developed for thin rectangular cross-sections and to refined higher-order plate theories for cylindrical bending displacement distributions provided that the Poisson ratio is set equal to zero. A finite element model has been developed using a partially weak formulation to ensure that the resulting boundary conditions represent physically meaningful quantities. Numerical results illustrate that the predicted displacements and stresses (including the parabolic shear stress distribution) are in a nearly exact agreement with existing elasticity solutions over a broad range of length aspect ratios ($3 \leqslant L/h \leqslant 1000$), boundary conditions and applied load definitions. Alternatively, the predicted displacement distributions for short deep beams using the Timoshenko beam theory can be very accurate, but these results are dependent upon the selected shear correction factor (k).

Acknowledgements—The support of this research by the National Science Foundation through grant MSM-8809132 is greatly appreciated.

REFERENCES

Bauchau, O. A. (1985). A beam theory for anisotropic materials. *J. Appl. Mech.* **52**, 416–422.

Cowper, G. R. (1966). The shear coefficient in Timoshenko's beam theory. *J. Appl. Mech.* **33**, 335–340.

Goodman, L. E. and Sutherland, J. G. (1951). Discussion of "Natural frequencies of continuous beams of uniform span length", by R. S. Ayre and L. S. Jacobson. *J. Appl. Mech.* **18**, 217–218.

Heyliger, P. R. and Reddy, J. N. (1988). A higher order beam finite element for bending and vibration problems. *J. Sound and Vibr.* **126**(2), 309–326.

Kaneko, T. (1975). On Timoshenko's correction for shear in vibrating beams. *J. Phys. D: Appl. Phys.* **8**, 1927–1936.

Kant, T. and Gupta, A. (1988). A finite element model for a higher-order shear-deformable beam theory. *J. Sound Vibr.* **125**(2), 193–202.

Kosmatka, J. B. and Dong, S. B. (1991). Saint-Venant solutions for prismatic anisotropic beams. *Int. J. Solids Structures* **28**(7), 917–938.

Levinson, M. (1981). A new rectangular beam theory. *J. Sound Vibr.* **74**(1), 81–87.

Love, A. E. H. (1927). *A Treatise on the Mathematical Theory of Elasticity*. Cambridge University Press, Cambridge, England.

Mason, W. E. and Herrmann, L. R. (1968). Elastic shear analysis of general prismatic beams. *J. Engng Mech. Div., Proc. ASCE* **94**, 965–983.

Michell, J. H. (1901). The theory of uniformly loaded beams. *Q. J. Math.* **32**, 28–42.

Reddy, J. N. (1984). A simple higher-order theory for laminated composite plates. *J. Appl. Mech.* **51**, 745–752.

Sokolnikoff, I. S. (1956). *Mathematical Theory of Elasticity*. McGraw-Hill, New York.

Tessler, A. and Dong, S. B. (1981). On a hierarchy of conforming Timoshenko beam elements. *Comp. Struct.* **14**, 335–344.

Timoshenko, S. P. (1921). On the correction for shear of the differential equation for transverse vibrations of prismatic bars. *Phil. Mag.* **41**, 744–746.

Timoshenko, S. P. (1922). On the transverse vibrations of bars of uniform cross-section. *Phil. Mag.* **43**, 125–131.

Timoshenko, S. P. and Goodier, J. N. (1970). *Theory of Elasticity*, 3rd Edn. McGraw-Hill, New York.

Vlasov, V. Z. (1961). *Thin-Walled Elastic Beams*. Israel Program for Scientific Translations Ltd, Jerusalem.

Wörndle, R. (1982). Calculation of the cross section properties and the shear stresses of composite rotor blades. *Vertica* **6**, 111–129.

APPENDIX

The moment resultants are defined as

$$S_1 = \int_A \sigma_z \psi_z \, \mathrm{d}A, \quad S_2 = \int_A \tau_{xz}\psi_{z,x} + \tau_{yz}\psi_{z,y} \, \mathrm{d}A, \tag{A1,2}$$

$$S_3 = \int_A \sigma_x \psi_{x,x} + \sigma_y \psi_{y,y} + \tau_{xy}(\psi_{x,y} + \psi_{y,x}) \, \mathrm{d}A, \quad S_4 = \int_A \tau_{xz}\psi_x + \tau_{yz}\psi_y \, \mathrm{d}A, \tag{A3,4}$$

the A_{ij} and the D_{ij} are defined as

$$A_{11} = a_9 + a_{12}, \quad A_{12} = a_{10} + a_{13}, \quad A_{22} = a_{11} + a_{14}, \tag{A5–7}$$

$$D_{11} = a_1 + a_3 + a_5 + a_7 + a_{15}, \quad D_{12} = a_7, \quad D_{22} = a_8, \tag{A8–10}$$

and finally, the stiffness submatrices and the force submatrices are defined as

$$[K_{vv}] = \int_0^L [a_{16}\{\phi_v'\}^{\mathrm{T}}\{\phi_v'\} - (a_{12} + a_{18})\{\phi_v\}^{\mathrm{T}}\{\phi_v''\} + a_8\{\phi_v\}^{\mathrm{T}}\{\phi_v''''\}] \, \mathrm{d}z, \tag{A11}$$

$$[K_{v\theta}] = \int_0^L [a_{16}\{\phi_v'\}^{\mathrm{T}}\{\phi_\theta\} + a_{17}\{\phi_v'\}^{\mathrm{T}}\{\phi_\theta''\} - (a_{18} + a_{12})\{\phi_v\}^{\mathrm{T}}\{\phi_\theta'\} + (a_7 - a_{13} - a_{19})\{\phi_v\}^{\mathrm{T}}\{\phi_\theta'''\}] \, \mathrm{d}z, \tag{A12}$$

$$[K_{\theta v}] = \int_0^L [(a_9 + a_{12})\{\phi_\theta\}^{\mathrm{T}}\{\phi_v'\} + (-a_2 - a_4 - a_8 + a_{10} + a_{13})\{\phi_\theta\}^{\mathrm{T}}\{\phi_v'''\} + a_6\{\phi_\theta'\}^{\mathrm{T}}\{\phi_v''\}] \, \mathrm{d}z, \tag{A13}$$

$$[K_{\theta\theta}] = \int_0^L [(a_9 + a_{12})\{\phi_\theta\}^{\mathrm{T}}\{\phi_\theta\} + a_5\{\phi_\theta'\}^{\mathrm{T}}\{\phi_\theta'\} + (a_{11} + a_{14})\{\phi_\theta\}^{\mathrm{T}}\{\phi_\theta''''\}$$
$$+ (-a_1 - a_3 - a_7 - a_{15} + 2a_{10} + 2a_{13})\{\phi_\theta\}^{\mathrm{T}}\{\phi_\theta''\}] \, \mathrm{d}z, \tag{A14}$$

$$\{f_v\} = \int_0^L p\{\phi_v\}^{\mathrm{T}} \, \mathrm{d}z, \quad \{f_\theta\} = -\bar{\psi}_x \int_0^L p'\{\phi_\theta\}^{\mathrm{T}} \, \mathrm{d}z, \tag{A15a, b}$$

where the constants a_1 through a_{19} are defined as:

$$a_1 = \int_A [(\lambda+2G)\psi_{x,x}^2 + \lambda(y+\psi_{y,y}+\psi_z)\psi_{x,x}]\,\mathrm{d}A, \quad a_2 = \int_A \lambda\psi_{x,x}\psi_z\,\mathrm{d}A, \tag{A16, 17}$$

$$a_3 = \int_A [(\lambda+2G)\psi_{y,y}^2 + \lambda(y+\psi_{x,x}+\psi_z)\psi_{y,y}]\,\mathrm{d}A, \quad a_4 = \int_A \lambda\psi_{y,y}\psi_z\,\mathrm{d}A, \tag{A18, 19}$$

$$a_5 = \int_A [(\lambda+2G)(y+\psi_z) + \lambda(\psi_{x,x}+\psi_{y,y})]y\,\mathrm{d}A, \quad a_6 = \int_A (\lambda+2G)y\psi_z\,\mathrm{d}A, \tag{A20, 21}$$

$$a_7 = \int_A [(\lambda+2G)(y+\psi_z) + \lambda(\psi_{x,x}+\psi_{y,y})]\psi_z\,\mathrm{d}A, \quad a_8 = \int_A (\lambda+2G)\psi_z^2\,\mathrm{d}A, \tag{A22, 23}$$

$$a_9 = \int_A G(1+\psi_{z,y})^2\,\mathrm{d}A, \quad a_{10} = \int_A G\psi_y(1+\psi_{z,y})\,\mathrm{d}A, \tag{A24, 25}$$

$$a_{11} = \int_A G\psi_y^2\,\mathrm{d}A, \quad a_{12} = \int_A G\psi_{z,x}^2\,\mathrm{d}A, \quad a_{13} = \int_A G\psi_x\psi_{z,x}\,\mathrm{d}A, \tag{A26–28}$$

$$a_{14} = \int_A G\psi_x^2\,\mathrm{d}A, \quad a_{15} = \int_A G(\psi_{x,y}+\psi_{y,x})^2\,\mathrm{d}A, \tag{A29, 30}$$

$$a_{16} = \int_A G(1+\psi_{z,y})\,\mathrm{d}A, \quad a_{17} = \int_A G\psi_y\,\mathrm{d}A, \tag{A31, 32}$$

$$a_{18} = \int_A G(1+\psi_{z,y})\psi_{z,y}\,\mathrm{d}A, \quad a_{19} = \int_A G\psi_y\psi_{z,y}\,\mathrm{d}A. \tag{A33, 34}$$